51-64

197133

N94-28674

Part 1

A MULTIGRID SOLVER FOR THE SEMICONDUCTOR EQUATIONS

Bernhard Bachmann

Institut für Angewandte Mathematik der Universität Zürich,
Rämistr.74, 8001 Zürich, Switzerland
and
Asea Brown Boveri, Corporate Research,
5405 Baden-Dättwil, Switzerland.

SUMMARY

We present a multigrid solver for the exponential fitting method, applied to the current continuity equations of semiconductor device simulation in two dimensions. The exponential fitting method is based on a mixed finite element discretization using the lowest-order Raviart-Thomas triangular element. This discretization method yields a good approximation of front layers and guarantees current conservation. The corresponding stiffness matrix is an M-matrix. "Standard" multigrid solvers, however, cannot be applied to the resulting system, as this is dominated by an unsymmetric part, which is due to the presence of strong convection in part of the domain. To overcome this difficulty, we explore the connection between Raviart-Thomas mixed methods and the nonconforming Crouzeix-Raviart finite element discretization. In this way we can construct nonstandard prolongation and restriction operators using easily computable weighted L^2-projections based on suitable quadrature rules and the upwind effects of the discretization. The resulting multigrid algorithm shows very good results, even for real-world problems and for locally refined grids.

1. INTRODUCTION

The exponential fitting method applied to the current continuity equations is based on a mixed finite element discretization using the lowest-order Raviart-Thomas triangular element [1]. This discretization yields a good approximation of front layers and guarantees current conservation. The corresponding scheme results in a large sparse system of equations, which is dominated by an unsymmetric part. When applying multigrid algorithms to the resulting system (7), the most difficult part is the construction of suitable prolongation and restriction operators. Using the connection between Raviart-Thomas mixed methods and the nonconforming Crouzeix-Raviart finite element discretization, we overcome this difficulty.

In § 2 we give some results from [2] concerning the mixed finite element discretization. We determine the resulting system and show the interrelation with a nonconforming finite element method. § 3 deals with the solution of the system of linear equations by our multigrid solver. First we construct easily computable L^2−projections, based on suitable quadrature rules and the upwind effect of the discretization. Due to the presence of strong convection in part of the domain it is also necessary to consider special smoothers for the multigrid algorithm. We use a minimal residual method with ILU preconditioning. The results of the numerical tests are given in § 4.

1

2. THE EXPONENTIAL FITTING METHOD FOR CURRENT CONTINUITY EQUATIONS

2.1. Mixed Finite Element Method

Let $\Omega \subset \mathbf{R}^2$ be a connected, bounded and polygonal domain. $H^m(\Omega)$, for $m \in \mathbf{N}$, and $L^2(\Omega) := H^0(\Omega)$ denote the usual Sobolev and Lebesque spaces equipped with the norm

$$\|u\|_m := \{\sum_{|\alpha| \le m} \int_\Omega |D^\alpha u|^2\}^{\frac{1}{2}}.$$

For $f \in L^2(\Omega)$ and $g \in L^2(\Gamma_0)$, $\Gamma_0 \subset \partial\Omega$ closed with positive length, we consider the current continuity equation, as given in [3]:

Find $u \in H^1(\Omega)$ such that

$$\begin{cases} \text{div } (\text{grad } u + u \text{ grad } \psi) = f & \text{in } \Omega \subset \mathbf{R}^2, \\ \qquad\qquad\qquad\quad u = g & \text{on } \Gamma_0 \subset \partial\Omega, \\ \dfrac{\partial u}{\partial n} + u\dfrac{\partial \psi}{\partial n} = 0 & \text{on } \Gamma_1 = \partial\Omega \setminus \Gamma_0. \end{cases} \tag{1}$$

The current is defined by $J = \text{grad } u + u \text{ grad } \psi$. Here, $\psi \in H^1(\Omega)$ is a given bounded function. To discretize problem (1) we introduce the classical method of changing variables from u to the socalled Slotboom variable ρ [3]

$$\rho = e^\psi u.$$

This results in the following symmetric form of problem (1):

Find $\rho \in H^1(\Omega)$ such that

$$\begin{cases} \text{div } (e^{-\psi}\text{grad } \rho) = f & \text{in } \Omega \subset \mathbf{R}^2, \\ \qquad\qquad\quad \rho = \chi := e^\psi g & \text{on } \Gamma_0 \subset \partial\Omega, \\ \dfrac{\partial \rho}{\partial n} = 0 & \text{on } \Gamma_1 = \partial\Omega \setminus \Gamma_0. \end{cases} \tag{2}$$

Let $\{\mathcal{T}_k\}_{k\ge0}$ be a regular sequence of decompositions of Ω into triangles. Denote by h_k the longest side of all triangles $T \in \mathcal{T}_k$. The set of edges of $\mathcal{T}_k$ is denoted by $\mathcal{E}_k$, where $\mathcal{E}_k^\partial$ are the boundary edges and $\mathcal{E}_k^0 = \mathcal{E}_k \setminus \mathcal{E}_k^\partial$ are all interelement boundaries. Denote by m_e the midpoint of an edge e of $\mathcal{E}_k$. Moreover, let P_m, $m \ge 0$, be the space of all polynomials of degree not greater than m. Following [1], we use the lowest order Raviart-Thomas mixed finite element to discretize (2). Therefore we define the following set of polynomial vectors

$$RT(T) := \{\tau = (\tau_1, \tau_2) : \tau_1 = \alpha + \beta x, \tau_2 = \gamma + \beta y, \ \alpha, \ \beta, \ \gamma \in \mathbf{R}\}, \quad \forall T \in \mathcal{T}_k,$$

and set

$$V_k := \{\tau \in (L^2(\Omega))^2 : \text{div } \tau \in L^2(\Omega), \ \tau\mathbf{n} = 0 \text{ on } \Gamma_1, \ \tau|_T \in RT(T) \ \forall T \in \mathcal{T}_k\},$$

$$W_k := \{\varphi \in L^2(\Omega) : \varphi|_T \in P_0(T) \ \forall T \in \mathcal{T}_k\}.$$

Then the mixed finite element discretization of (2) is defined as:

Find $(\mathbf{J_k}, \rho_k) \in V_k \times W_k$ such that for all $(\tau_k, \varphi_k) \in V_k \times W_k$

$$\begin{cases} \int_\Omega e^\psi \mathbf{J_k}\tau_k dx + \int_\Omega \rho_k \text{div } \tau_k dx = \int_{\Gamma_0} \chi\tau_k \mathbf{n} ds, \\ \int_\Omega \varphi_k \text{div } \mathbf{J_k} dx \qquad\qquad = \int_\Omega f\varphi_k dx. \end{cases} \qquad (3)$$

The matrix associated with (3) is not coercive. To avoid this inconvenience we introduce a Lagrange multiplier. We define

$$\tilde{V}_k := \{\tau \in (L^2(\Omega))^2 : \tau|_T \in RT(T) \ \forall T \in \mathcal{T}_k\},$$

and for $\xi \in L^2(\Gamma_0)$

$$\Lambda_{k,\xi} := \{\mu : \mu \in L^2(\mathcal{E}_k), \ \mu|_e \in P_0(e) \ \forall e \in \mathcal{E}_k, \ \int_e (\mu - \xi) ds = 0 \ \forall e \subset \Gamma_0\}.$$

Instead of (3) we now consider the mixed equilibrium discretization,

Find $(\tilde{\mathbf{J}}_k, \tilde{\rho}_k, \lambda_k) \in \tilde{V}_k \times W_k \times \Lambda_{k,\chi}$ such that for all $(\tau_k, \varphi_k, \mu_k) \in \tilde{V}_k \times W_k \times \Lambda_{k,0}$

$$\begin{cases} \int_\Omega e^\psi \tilde{\mathbf{J}}_k \tau_k dx + \sum_{T \in \mathcal{T}_k} \int_T \tilde{\rho}_k \text{div } \tau_k dx - \sum_{T \in \mathcal{T}_k} \int_{\partial T} \lambda_k \tau_k \mathbf{n} ds = 0, \\ \sum_{T \in \mathcal{T}_k} \int_T \varphi_k \text{div } \tilde{\mathbf{J}}_k dx \qquad\qquad\qquad = \int_\Omega f\varphi_k dx, \\ \sum_{T \in \mathcal{T}_k} \int_{\partial T} \mu_k \tilde{\mathbf{J}}_k \mathbf{n} ds \qquad\qquad\qquad = 0. \end{cases} \qquad (4)$$

As shown in [3], problem (4) has a unique solution and $\mathbf{J_k} \equiv \tilde{\mathbf{J}}_k$, $\rho_k \equiv \tilde{\rho}_k$ holds. Moreover, λ_k is a good approximation of the solution of (2) at the interelement boundaries [2]. It is possible to eliminate the unknowns, corresponding to $\tilde{\mathbf{J}}_k$ and $\tilde{\rho}_k$ in the resulting system, by static condensation [3]. This yields a matrix (acting only on the interelement multiplier λ_k), which is a symmetric positive definite matrix and which is an M-matrix if the triangulation is of the weakly acute type (i.e. no angle $> \frac{\pi}{2}$).

3

2.2. The Nonconforming Finite Element Formulation

To introduce the nonconforming finite element formulation we need the following definitions: Let Π_k^0 be the L^2–projection from $L^2(\mathcal{E}_k)$ onto

$$\Lambda_k := \{\mu_k \in L^2(\mathcal{E}_k) : \mu_k|_e \in P_0(e) \ \forall e \in \mathcal{E}_k\}$$

and P_k^0 be the L^2–projection from $L^2(\Omega)$ onto

$$\tilde{S}_k := \{v_k \in L^2(\Omega) : v_k|_T \in P_0(T) \ \forall T \in \mathcal{T}_k\},$$

i.e. $\quad \Pi_k^0(\xi)|_e = \dfrac{1}{|e|} \displaystyle\int_e \xi ds, \quad \forall e \in \mathcal{E}_k \quad \text{and} \quad P_k^0(u)|_T = \dfrac{1}{|T|} \displaystyle\int_T u dx, \quad \forall T \in \mathcal{T}_k.$

The Crouzeix-Raviart finite element space [4] is defined by

$$S_k := \{v_k \in L^2(\Omega) : v_k|_T \in P_1(T) \ \forall T \in \mathcal{T}_k, \ v_k \text{ is continuous at midpoints of edges}\}.$$

For $\xi \in L^2(\Gamma_0)$ we define

$$S_{k,\xi} := \{v_k \in S_k : v_k(m_e) = \Pi_k^0(\xi)|_e, \ e \subset \Gamma_0\}.$$

Notice that the standard basis functions of S_k are equal to one at the midpoint of exactly one edge and vanish at the midpoints of all other edges. Using the arguments concerning static condensation in [5], it is straightforward to prove the following lemma.

Lemma 2.1.

The solution λ_k of (4) can be written as $\lambda_k = \Pi_k^0(w_k)$, where w_k is the solution of the following nonconforming weak problem

Find $w_k \in S_{k,\chi}$ such that for all $v_k \in S_{k,0}$

$$\sum_{T \in \mathcal{T}_k} (P_k^0(e^\psi))^{-1} \int_T \operatorname{grad} w_k \operatorname{grad} v_k dx = \sum_{T \in \mathcal{T}_k} P_k^0(f) \int_T \left(\frac{3}{2} - \frac{1}{2}\frac{e^\psi}{P_k^0(e^\psi)}\right) v_k dx. \tag{5}$$

$\diamond$

Remark 2.2.

For w_k as in Lemma 2.1. and the solution ρ of (2) the following error estimate [2] holds:

$$\|\rho - w_k\|_0 \leq \gamma |h_k|^2 (\|\rho\|_3 + \|\mathbf{J}\|_2)$$

with $\gamma = \gamma(e^\psi)$ independent of ρ and h_k.

$\diamond$

The Lagrange multiplier λ_k is an approximation of $\rho = e^{\psi} u$. In semiconductor simulations the range of ψ is very large, so that λ_k is not suited for actual computations. Moreover we are interested in approximating the solution u of (1). Hence we introduce the following change of variable

$$\mu_k = (\Pi_k^0(e^{\psi}))^{-1} \lambda_k \in \Lambda_{k,(\Pi_k^0(e^{\psi}))^{-1}\chi}. \tag{6}$$

Denote the standard basis of S_k by φ_e, $e \in \mathcal{E}_k$. We define the linear operator $E_k : S_k \to S_k$ by

$$E_k(\varphi_e) = \Pi_k^0(e^{\psi})|_e \varphi_e \quad \forall e \in \mathcal{E}_k.$$

For $f \in L^2(\Omega)$, $G_k(f) \in L^2(\Omega)$ is defined by

$$G_k(f) = P_k^0(f)\left(\frac{3}{2} - \frac{1}{2}\frac{e^{\psi}}{P_k^0(e^{\psi})}\right).$$

Finally we arrive at the following statement:

Lemma 2.3.

Let $\zeta = (\Pi_k^0(e^{\psi}))^{-1}\chi \in L^2(\Gamma_0)$. Then μ_k of (6) can be written as $\mu_k = \Pi_k^0(u_k)$, where u_k is the solution of the nonconforming weak problem:

Find $u_k \in S_{k,\zeta}$ such that for all $v_k \in S_{k,0}$

$$\sum_{T \in \mathcal{T}_k} (P_k^0(e^{\psi}))^{-1} \int_T \operatorname{grad} E_k(u_k) \operatorname{grad} v_k dx = \int_{\Omega} G_k(f) \, v_k dx. \tag{7}$$

◇

Remark 2.4.

Note that problem (7) is the usual nonconforming Crouzeix-Raviart discretization of the Laplace equation, if ψ and f are constant on Ω.

◇

We can use the error estimate of Remark 2.2. to obtain an estimate for the approximation error between the solution u_k from (7) and the solution u of (1), though the result is rather unsatisfying. To arrive at an improved error bound, one could use the fact that two Babuška-Brezzi conditions hold [6] for the corresponding bilinear form. The stability and the unique solvability of the discrete problem (7) also follow. In the following we construct a multigrid algorithm for problem (7). Therefore we define the bilinear form a_k on S_k by

$$a_k(u_k, v_k) := \sum_{T \in \mathcal{T}_k} (P_k^0(e^{\psi}))^{-1} \int_T \operatorname{grad} E_k(u_k) \operatorname{grad} v_k \, dx.$$

3. MULTIGRID METHOD

3.1. Adaptive Mesh-Refinement Techniques

In order to formulate the multigrid algorithm, we need a regular sequence of triangulations $\{\mathcal{T}_k\}_{k \geq 0}$. In our refinement process, two objectives are pursued. First, in order to improve approximation, we should refine the grid locally, where the solution behaves very badly. Second, we have to construct weakly acute triangulations to guarantee that the corresponding discretization matrix is an M-matrix. Therefore we define the strategy and rules below. Given a triangulation we refine its triangles as follows:

(1) The refinement process is started by a suitable error estimator, e.g. based on residuals, which marks some of the triangles as red.

(2) If a triangle is marked

    (i) *red*, it will be cut into four new ones by joining the midpoints of its edges,

    (ii) *green*, it will be cut into two new triangles by joining the midpoint of the longest edge to the vertex opposite to this edge, and

    (iii) *blue*, it will be cut into three new triangles by joining the midpoint of its longest edge to the vertex opposite to this edge and to the midpoint of one of the remaining edges (see Fig.1)
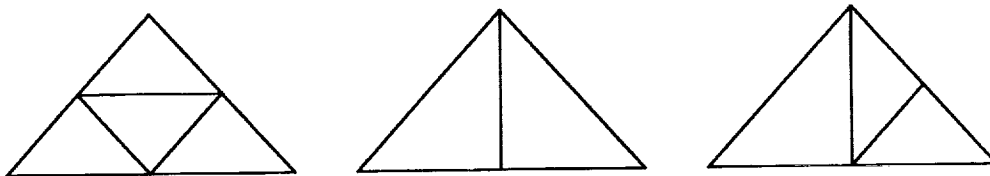

Figure 1. Red, green and blue refinement of a triangle.

(3) Hanging nodes are avoided using the following rules:

    (i) a triangle with three hanging nodes is marked *red*

    (ii) a triangle with two hanging nodes is marked *blue*, if one of the nodes lies on the longest edge of the triangle; otherwise it is marked *red*

    (iii) a triangle with one hanging node is marked *green*, if the node lies on the longest edge of the triangle; otherwise it is marked *blue*

Note that rules (ii) and (iii) may introduce new hanging nodes. However, one can prove that the refinement process obeying the above rules is finite. Moreover, assuming that $\mathcal{T}_0$ has only isosceles right-angled triangles, then it is guaranteed that all triangulations $\mathcal{T}_k$ are weakly acute.

3.2. The Prolongation

In order to solve problem (1), we have to find the solution u_k of the discrete problem (7). Since the Crouzeix-Raviart element is nonconforming and $S_{k-1} \not\subset S_k$, we must construct a suitable transfer operator between S_{k-1} and S_k. In addition, the discretization shows upwind effects due to the existence of strong convection in part of the domain. This also must be taken into account.

In [7, 8] a hierarchical basis multigrid method was used to solve a linear system arising from the convection diffusion equation by an upwind discretization. It was shown that the convergence of the hierarchical basis multigrid method depends on the strength of the convection term. When solving the discrete problem (7) with the multigrid algorithm [9], a similar effect can be seen in the numerical experiments. On the other hand, considering the one dimensional problem, one sees that a good interpolation has to regard the upwind effect. Therefore we introduce the following weighted L^2-projection. Define

$$(u,v)_k := \sum_{\tilde{T} \in \mathcal{T}_k} (P_k^0(e^\psi)|_{\tilde{T}})^{-1} \sum_{\substack{T \in \mathcal{T}_{k+1} \\ T \subset \tilde{T}}} \int_T E_k(u)\, v dx \quad \forall\, u \in S_k,\ v \in S_k \cup S_{k+1}. \tag{8}$$

For all $u \in P_2(T)$, $T \in \mathcal{T}_k$, the quadrature rule

$$\int_T u dx = \frac{|T|}{3} \sum_{e \subset \partial T} u(m_e)$$

is exact, so that (8) can be written as

$$(u,v)_k = \sum_{\tilde{T} \in \mathcal{T}_k} (P_k^0(e^\psi)|_{\tilde{T}})^{-1} \sum_{\substack{T \in \mathcal{T}_{k+1} \\ T \subset \tilde{T}}} \frac{|T|}{3} \sum_{e \subset \partial T} E_k(u)(m_e)\, v(m_e) \tag{9}$$

for all $u \in S_k$ and $v \in S_k \cup S_{k+1}$.

Remark 3.1.

Note that if $v \in S_k$ holds, (9) reduces to the equation

$$(u,v)_k = \sum_{\tilde{T} \in \mathcal{T}_k} (P_k^0(e^\psi)|_{\tilde{T}})^{-1} \frac{|\tilde{T}|}{3} \sum_{e \subset \partial \tilde{T}} \Pi_k^0(e^\psi)|_e\, u(m_e)\, v(m_e).$$

Moreover, if ψ is constant, we have

$$(u,v)_k = (u,v) \quad \forall\, u \in S_k,\ v \in S_k \cup S_{k+1},$$

where $(u,v) := \int_\Omega uv\, dx$ denotes the usual L^2-inner product.

From (9) it follows that the standard basis functions of S_k are mutually orthogonal with respect to the inner product $(.,.)_k$. Therefore we can obtain an easily computable prolongation operator $P_{k-1}^k : S_{k-1} \to S_k$ by

$$(P_{k-1}^k u_{k-1}, v_k)_k = (u_{k-1}, v_k)_{k-1} \quad \forall\, u_{k-1} \in S_{k-1},\ v_k \in S_k.$$

It is straightforward to prove the following lemma:

Lemma 3.2.

Let $u_{k-1} \in S_{k-1}$, then:

If $e \in \mathcal{E}_k^\partial$ then $(P_{k-1}^k u_{k-1})(m_e) = \left(\dfrac{\Pi_k^0(e^\psi)|_e}{P_k^0(e^\psi)|_T}\right)^{-1} \dfrac{(E_{k-1}u_{k-1})(m_e)|_{\tilde{T}}}{P_{k-1}^0(e^\psi)|_{\tilde{T}}}$,

where T (resp. $\tilde{T}$) is the triangle in $\mathcal{T}_k$ (resp. $\mathcal{T}_{k-1}$) with $e \subset \partial T$ (resp. $e \subset \partial \tilde{T}$).

If $e \in \mathcal{E}_k^0$ then

$$(P_{k-1}^k u_{k-1})(m_e) = \left(|T^L|\frac{\Pi_k^0(e^\psi)|_e}{P_k^0(e^\psi)|_{T^L}} + |T^R|\frac{\Pi_k^0(e^\psi)|_e}{P_k^0(e^\psi)|_{T^R}}\right)^{-1}$$
$$\left(|T^L|\frac{(E_{k-1}u_{k-1})(m_e)|_{\tilde{T}^L}}{P_{k-1}^0(e^\psi)|_{\tilde{T}^L}} + |T^R|\frac{(E_{k-1}u_{k-1})(m_e)|_{\tilde{T}^R}}{P_{k-1}^0(e^\psi)|_{\tilde{T}^R}}\right),$$

where T^L, T^R (resp. $\tilde{T}^L, \tilde{T}^R$) are the two triangles in $\mathcal{T}_k$ (resp. $\mathcal{T}_{k-1}$) with $T^L \cap T^R = e$ and $T^L \subset \tilde{T}^L$, $T^R \subset \tilde{T}^R$. (see Fig.2)

$\diamond$

Remark 3.3.

If ψ of Lemma 3.2 is constant, we have the usual L^2−projection I_{k-1}^k as given in [9]. The coefficients $\dfrac{\Pi_k^0(e^\psi)|_e}{P_k^0(e^\psi)|_T}$, $k \geq 0$, are also computed during the construction of the stiffness matrix, hence the interpolation is not very expensive. On the other hand, as shown in [5] the coefficients $\dfrac{\Pi_k^0(e^\psi)|_e}{P_k^0(e^\psi)|_T}$, $k \geq 0$, introduce an upwind effect; i.e. the coefficient corresponding to the downwind node is equal to zero.

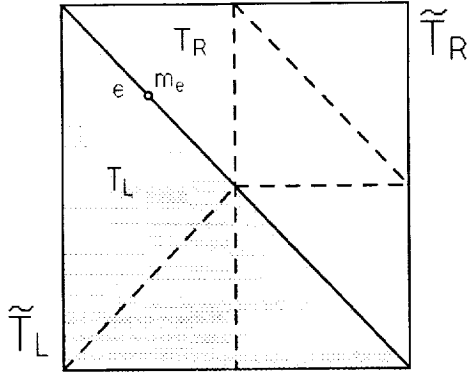$\diamond$

Figure 2. Interpolation.

3.3. The Smoother

A suitable smoother for the system (7) is given in [10] by a Gauss-Seidel-iteration with decoupling. This smoother is confined to special triangulations and does not allow adaptive grid refinements. Another candidate for problems with strong convection terms is the ILU-iteration. Here we restrict ourselves to a variant of the ILU-iteration. The ILU-decomposition of the linear system A_k, related to problem (7) and the standard basis of the Crouzeix-Raviart finite element space $S_{k,\zeta}$, can be written as

$$A_k = L_k U_k - D_k,$$

where L_k, U_k and D_k are given by the sparsity pattern of A_k. Denote by $\alpha_k = (\alpha_e)_{e \in \mathcal{E}_k}$ the coefficient vector of $u_k = \sum_{e \in \mathcal{E}_k} \alpha_e \varphi_e \in S_{k,\zeta}$ and by b_k the right hand side. Then the ILU-iteration is given by:

$$\alpha_k^0 \text{ an arbitrary starting vector, } w \in (0,1],$$
$$\alpha_k^i = \alpha_k^{i-1} + \omega (L_k U_k)^{-1}(b_k - A_k \alpha_k^{i-1}), \quad \forall i = 1, \cdots.$$

In order to get a good smoothing rate, we must optimize the factor

$$\frac{\|A_k(\alpha_k^i - \alpha_k^*)\|_2}{\|A_k(\alpha_k^0 - \alpha_k^*)\|_2},$$

as mentioned in [11]. Here α_k^* is the solution of $A_k \alpha_k = b_k$. Therefore, by computing the optimal damping parameter ω in every step, our final smoothing algorithm is

Algorithm 3.4.

α_k^0 an arbitrary starting vector, $r_k^0 = b_k - A_k \alpha_k^0$,

for $i = 1, \cdots,$ compute:

$$d_k^{i-1} = (L_k U_k)^{-1} r_k^{i-1},$$

$$v_k^{i-1} = A_k d_k^{i-1},$$

$$\omega^{i-1} = \frac{v_k^{i-1^T} r_k^{i-1}}{v_k^{i-1^T} v_k^{i-1}},$$

$$\alpha_k^i = \alpha_k^{i-1} + \omega^{i-1} d_k^{i-1},$$

$$r_k^i = r_k^{i-1} - \omega^{i-1} v_k^{i-1},$$

end.

◇

Remark 3.5.

Algorithm 3.4. can be interpreted as a minimal residual method with ILU-preconditioning.

◇

3.4. Multigrid Algorithm

Now we are in the position to formulate our multigrid algorithm.

Algorithm 3.6. (One MG-iteration at level k)

(1) *Pre-smoothing:* Given $u_k^0 = \sum_{e \in \mathcal{E}_k} \alpha_e^0 \varphi_e \in S_{k,\zeta}$. For $i = 1, \cdots, \nu_1$ compute u_k^i, using Algorithm 3.4.

(2) *Coarse-Grid Correction:* Denote by $u_{k-1}^* \in S_{k-1,0}$ the solution of the coarse grid problem

$$a_{k-1}(u_{k-1}, v_{k-1}) = (G_k(f), I_{k-1}^k v_{k-1}) - a_k(u_k^{\nu_1}, I_{k-1}^k v_{k-1}) \quad \forall v_{k-1} \in S_{k-1,0}. \tag{$*$}$$

If $k = 1$, set $\tilde{u}_{k-1} = u_{k-1}^*$. If $k > 1$, compute an approximation $\tilde{u}_{k-1}$ to u_{k-1}^* by applying $\mu = 1$ or $\mu = 2$ iterations of the algorithm at level $k - 1$ to problem $(*)$ and starting value 0. Set

$$u_k^{\nu_1 + 1} := u_k^{\nu_1} + P_{k-1}^k \tilde{u}_{k-1}.$$

(3) *Post-smoothing:* Apply ν_2 iterations of Algorithm 3.4. to $u_k^{\nu_1 + 1}$.

◇

Remark 3.7.

So far, there exists no convergence proof for Algorithm 3.6. The standard convergence analysis, as in [9, 11], cannot be used here, because the bilinear form $a_k(.,.)$ is unsymmetric.

◇

4. NUMERICAL RESULTS

In this section we present three numerical examples which demonstrate the behaviour of the proposed multigrid method. In all experiments we measure the performance of a method by the arithmetic mean of the convergence rates

$$\rho_i = \sqrt[i]{\frac{r_k^{iT} r_k^i}{r_k^{0T} r_k^0}},$$

where r_k^i is the defect of the i-th iteration.

The first model problem is taken from the papers of Brezzi, Marini and Pietra [3, 5]. We consider the domain $\Omega := (0,1) \times (0,1)$ with Neumann boundary

$$\Gamma_1 := \{(x,y) : ((x = 1) \wedge (y < 0.75)) \vee ((y = 1) \wedge (x < 0.75))\}$$

and Dirichlet boundary $\Gamma_0 := \partial\Omega \setminus \Gamma_1$, right hand side $f \equiv 0$ and potential ψ defined as $\psi(x,y) := \dfrac{\psi_0(x,y)}{l}$ with

$$\psi_0(x,y) := \begin{cases} 0.0 & \text{if} \quad 0.0 \leq r \leq 0.8 \\ r - 0.8 & \text{if} \quad 0.8 \leq r \leq 0.9 \\ 0.1 & \text{if} \quad 0.9 \leq r \end{cases} \quad \text{with } r := \sqrt{(x-1)^2 + (y-1)^2}.$$

On Γ_0 we have $g(x,y) = 0$ if $x = 0$ or $y = 0$ and $g(x,y) = 1$ otherwise. We use the initial triangulation $\mathcal{T}_0$ as given in Fig.3. and refine every triangulation by marking all triangles as red (uniform refinement). The numerical solution for $l = 10^6$ and a locally refined grid is shown in Fig.4.
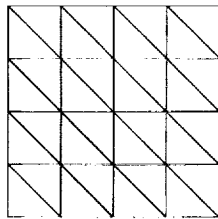

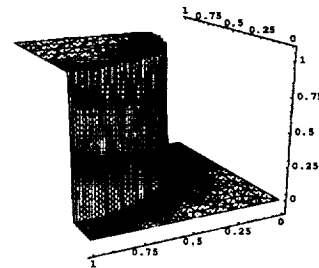Figure 3. Initial triangulation 1.

Figure 4. Numerical Solution.

We test our multigrid algorithm 3.6. with two pre- and two post-smoothing steps ($\nu_1 = \nu_2 = 2$) and with different values of μ (only smoothing : $\mu = 0$; V-cycle : $\mu = 1$; W-cycle : $\mu = 2$) for problems with varying k_{max} ($k_{max} = 1, \cdots, 5$). The corresponding convergence rates for $l = 10$ and $l = 10^6$ are given in Tab.1 and Tab.2 respectively. In all experiments we used the same arbitrary starting vector.

k_{max}	1	2	3	4	5
$\mu = 0$	.672	.854	.886	.904	.910
$\mu = 1$	.032	.103	.159	.208	.253
$\mu = 2$	.032	.074	.059	.059	.055

Table 1. Convergence rates ($l = 10$)

k_{max}	1	2	3	4	5
$\mu = 0$	.736	.879	.890	.906	.910
$\mu = 1$	.096	.245	.358	.427	.482
$\mu = 2$	.096	.221	.266	.235	.201

Table 2. Convergence rates ($l = 10^6$)

In Tab.3 we show the results for $k_{max} = 5$ and with varying μ and $l = 10^m$.

m	0	1	2	3	4	5	6
$\mu = 0$	.907	.910	.908	.906	.908	.910	.908
$\mu = 1$	.227	.253	.444	.473	.483	.482	.482
$\mu = 2$	.053	.055	.075	.174	.198	.201	.201

Table 3. Convergence rates ($k_{max} = 5$)

In the second experiment we take

$$f = -2 \ 10^5 \frac{e^{-\psi(x,y)}}{(\cosh(100 \ (r - 0.65)))^2},$$

with $\psi(x,y) = 10^3 \ (1 + \tanh(100 \ (r - 0.65)))$ and $r = \sqrt{(x - 1)^2 + (y - 1)^2}$. Again we chose $\Omega = (0,1) \times (0,1)$. The Dirichlet boundary $\Gamma_0 = \partial\Omega$ and $g(x,y) = (x + y) \ e^{-\psi(x,y)}$. The exact solution is given by

$$u(x,y) = (x + y) \ e^{-\psi(x,y)}.$$

The numerical solution is shown in Fig.7. We used three different coarse grids, as given in Fig.3, Fig.5 and Fig.6, to show that the Algorithm 3.6. does not depend on the orientation of the grid. For uniform refinement and $k_{max} = 5$ Tab.4 shows the results with varying μ ($\mu = 0, 1, 2$). In Tab.4 we also show the results for $k_{max} = 6$ and adaptive refinement of the grid (see Fig.8).
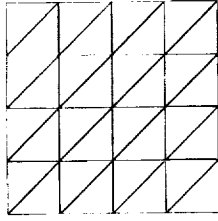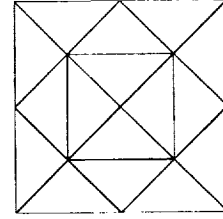
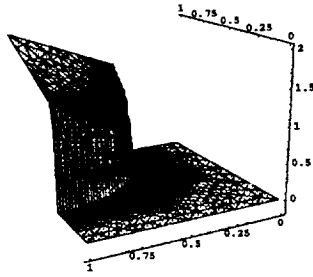Figure 5. Initial triangulation 2.

Figure 6. Initial triangulation 3.

Figure 7. Numerical solution.
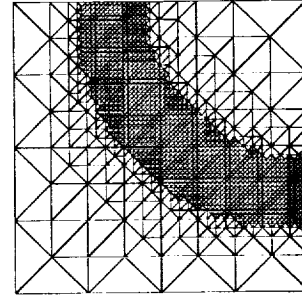
Figure 8. Adaptive refined grid ($k = 4$).

grid	init. triang. 1	init. triang. 2	init. triang. 3	loc. ref.
$\mu = 0$	.900	.903	.891	.905
$\mu = 1$	.311	.225	.216	.409
$\mu = 2$	.157	.087	.128	.355

Table 4. Convergence rates

Finally we consider an experiment with a real-world problem. Fig.9 shows the schematic structure of the doping of a thyristor. With an existing simulation program (ABBPISCES) we computed the solution u of (1) and the potential ψ of the coupled stationary semiconductor equations for a blocking-state (see Fig.11 resp. Fig.12) and an on-state of the thyristor (see Fig.13 resp. Fig.14). The so computed potential ψ was substituted into equation (1) and the resulting system was solved with our multigrid algorithm. Fig.10 shows the grid for an adaptive refinement ($k = 5$). Finally Tab.5 shows the convergence rates for Algorithm 3.6. with a suitable number of pre- and post-smoothing steps, with varying μ ($\mu = 0, 1, 2$) and $k_{max} = 7$.
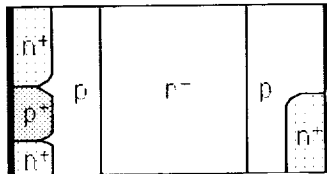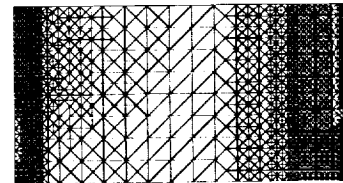

Figure 9. Schematic structure of the doping.

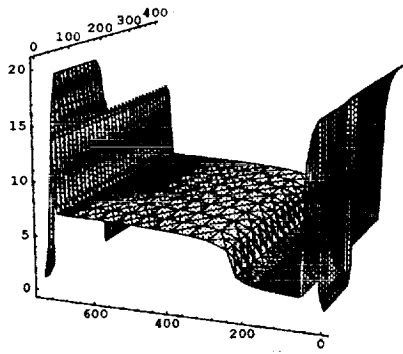Figure 10. Adaptive grid ($k = 5$).

Figure 11. Solution (log).
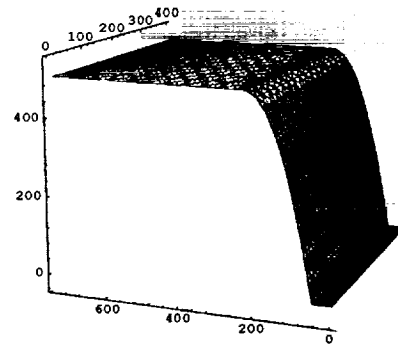
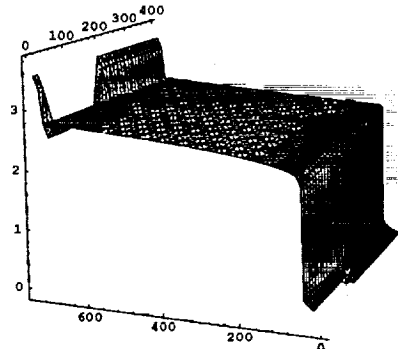Figure 12. Potential.
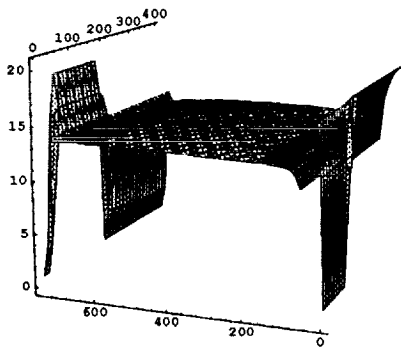
Figure 13. Solution (log).

Figure 14. Potential.

state	blocking	on
$\mu = 0$	.843	.828
$\mu = 1$ $(\nu_1 = \nu_2 = 22)$	.249	.112
$\mu = 2$ $(\nu_1 = \nu_2 = 9)$	.108	.121

Table 5. Convergence rates

5. REFERENCES

1. Raviart, P.-A.; and Thomas, J.M.: A mixed finite element method for second order elliptic problems, *Mathematical Aspects of the Finite Element Method,* Lecture Notes in Mathematics, 606, Springer, Berlin, 1977, pp. 292-315.

2. Arnold, D.N.; and Brezzi, F.: Mixed and nonconforming finite element methods, postprocessing and error estimates, *RAIRO M^2AN,* vol.19, 1985, pp. 7-32.

14

3. Brezzi, F.; Marini, L.D.; and Pietra, P.: Two-dimensional exponential fitting and application to drift-diffusion models, *SIAM J. Numer. Anal.*, vol.26, 1989, pp. 1342-1355.

4. Crouzeix, M.; and Raviart, P.A.: Conforming and non-conforming finite element methods for solving the stationary Stokes equation, *RAIRO Anal. Numér.*, vol.7, 1973, pp. 33-76.

5. Brezzi, F.; Marini, L.D.; and Pietra, P.: Numerical simulation of semiconductor devices, *Comp. Meths. Appl. Mech. Engr.*, vol.75, 1989, pp. 493-513.

6. Bachmann, B.: *Adaptive Mehrgitterverfahren zur Lösung der stationären Halbleitergleichungen*, Dissertation, Universität Zürich, 1993.

7. Bank, R.E.; and Benbourenane, M.: A Fourier analysis of the two-level hierarchical basis multigrid method for convection-diffusion equations, *Proceedings of the Fourth International Symposium on Domain Decomposition Methods for Partial Differential Equations*, SIAM, Philadelphia, 1991, pp. 178-184.

8. Bank, R.E.; and Benbourenane, M.: The hierarchical basis multigrid method for convection-diffusion equations, *Numer. Math.*, vol.61, 1992, pp. 7-37.

9. Braess, D.; and Verfürth, R.: Multi-grid methods for non-conforming finite element methods, *SIAM J. Numer. Anal.*, vol.27, 1990, pp. 979-986.

10. Reusken, A.: Multigrid applied to mixed finite element schemes for current continuity equations, University Eindhoven, RANA 90-13, Nov. 1990.

11. Hackbusch, W.: *Multi-Grid Methods and Applications*, Springer, Berlin-Heidelberg, 1985.